PAPER Nr. : 1

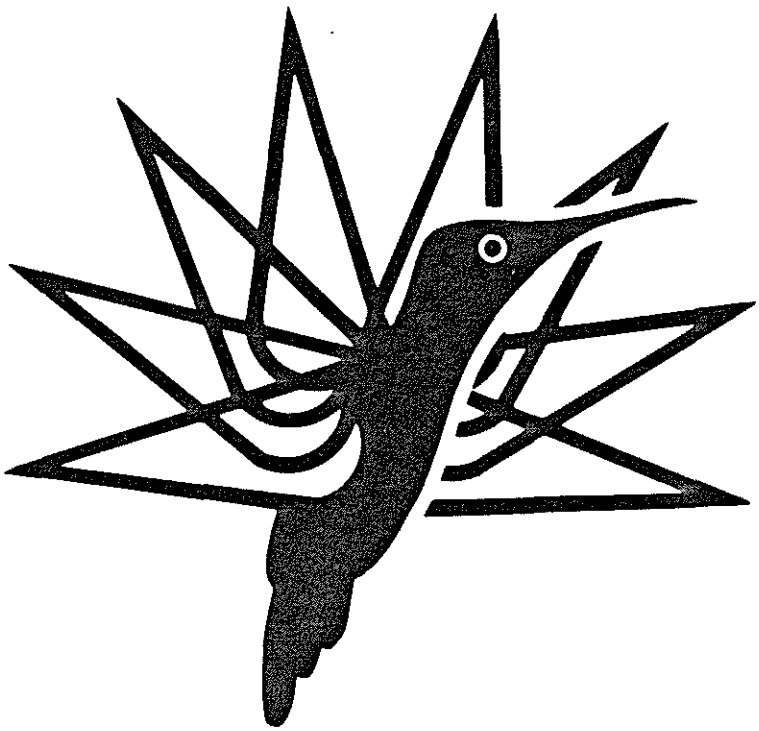

IMPROVEMENT OF TWO BLADE SECTIONS FOR HELICOPTER ROTORS

BY

K.H. HORSTMANN, H. KÖSTER

DEUTSCHE FORSCHUNGS- UND VERSUCHSANSTALT FÜR LUFT- UND RAUMFAHRT (DFVLR)
BRAUNSCHWEIG, GERMANY

AND

G. POLZ

MESSERSCHMITT-BÖLKOW-BLOHM GMBH

MÜNCHEN, GERMANY

TENTH EUROPEAN ROTORCRAFT FORUM

AUGUST 28 – 31, 1984 – THE HAGUE, THE NETHERLANDS

IMPROVEMENT OF TWO BLADE SECTIONS FOR HELICOPTER ROTORS

K.H. HORSTMANN, H. KÖSTER
DEUTSCHE FORSCHUNGS- UND VERSUCHSANSTALT FÜR LUFT- UND RAUMFAHRT e.V. (DFVLR)
BRAUNSCHWEIG, GERMANY

G. POLZ
MESSERSCHMITT-BÖLKOW-BLOHM GMBH
MÜNCHEN, GERMANY

Abstract

In cooperation between DFVLR and MBB two new advanced airfoils for helicopter rotor blades have been developed. In a second step these airfoils are now improved by further theoretical and experimental investigations. For the inner airfoil higher maximum lift coefficients at low Mach numbers could be obtained and for the tip airfoil the drag rise Mach numbers could be increased. Some design aspects are discussed and the main experimental results are presented. Some rotor performance calculations show the improvement of rotor efficiency by these new airfoils.

1. Introduction

The nessecity of improving the aerodynamics of helicopters in order to increase cruise speed and payloads and to decrease the fuel consumption has clearly been seen by helicopter manufacturers and they made big efforts in this area for at least fifteen years. One of the most essential task was the improvement of the rotor performance first by using composite materials which allows the design of rotor blades with a spanwise evolution of the blade's sections and second by the application of new airfoil shapes.

Since the end of the sixties and the beginning of the seventies research work on transonic airfoils for wings has been raised to get a better understanding of the flow phenomena and to develop more reliable and simpler calculation methods. As helicopter rotor blade sections pass flow regimes in which regions of supersonic flow on the airfoil contour occur, this advanced knowledge has been used for developing improved rotor blade sections. In ref.[1] to [11] the problems of rotor airfoils are discussed in detail and some results of these efforts are given.

In 1981 a cooperation has been started between the Institute for Design Aerodynamics of DFVLR and the Helicopter Division of MBB for developing advanced airfoils for new helicopter rotors. Two airfoils have been designed which are designated by DM-H1 Tb and DM-H2 Tb and have been investigated in the Transonic Wind Tunnel Braunschweig of DFVLR [12]. These airfoils fulfilled almost completely the stated requirements in regard to aerodynamic performances and moment behaviour.

The experience which has been gained during the design process of the new airfoils and the comparison of theoretical and experimental results offered the possibility to improve or to change some characteristics of these airfoils in view of a higher degree of adaption to rotor requirements. In order to realize the possible improvements the airfoils have been modified in a second development step.

2. Features of airfoil improvement

Depending on the mission profiles of a rotor aircraft a lot of parameters have to be specified determining the operational conditions of a blade section:

- rotor tip speed
- radial position of a blade section
- blade twist distribution
- rotor disc area loading
- rotor solidity
- inclination of the blade tip plane
- flight speed

The influence of some of these parameters on airfoil design has been discussed in ref. [12]. The main airfoil requirements for different flight conditions of a transport rotorcraft at the radial blade positions r/R = 0.8 and 0.95 are summarized as design objectives in following table:

design objective	inner airfoil	tip airfoil
thickness ratio t/c	12%	9%
drag divergence	$M_{DDo} > 0.79$	$M_{DDo} > 0.84$
drag at M = 0.6, c_L=0.7	$c_D \leqq 0.01$	$c_D \leqq 0.01$
maximum lift at M = 0.3 M = 0.4 M = 0.5	$c_{L\,max}$ = 1.5 1.45 1.3	c_{Lmax} = 1.3 1.2
pitching moment below stall inception	$\lvert c_m \rvert \leqq 0.01$	$\lvert c_m \rvert \leqq 0.01$

In the figs.1 and 2 the design objectives and the main operational conditions of the two blade sections are characterized by the shaded areas. Additionally the measured performance boundaries of the airfoils DM-H1 Tb and DM-H2 Tb are included. The stated requirements are completely fulfilled except in the case of maximum lift at the Mach number M = 0.4 of the airfoil DM-H2 Tb for inner blade positions, fig. 1. The dent to lower values in the maximum lift coefficient curve in this important Mach number range reduces the airfoil performances noticeably.

In the range of zero or small negative lift coefficients at high Mach numbers for the airfoil DM-H1 Tb, fig. 2, the design requirements are fulfilled too. But due to the high dynamic pressure at the tip of the advancing blade and the high drag caused thereby it is desirable to shift the drag rise to somewhat higher Mach numbers. This can be realized by slightly reducing the maximum lift coefficients of the airfoil DM-H1 Tb which are higher than stated by the design objectives.

The advantage to change the DM-H1 Tb and DM-H2 Tb airfoil performances in the manner discussed above can also be seen in fig. 3, showing the maximum lift coefficient of several airfoils at the Mach number M = 0.4 versus drag divergence Mach number at zero lift coefficient. The values of the airfoils

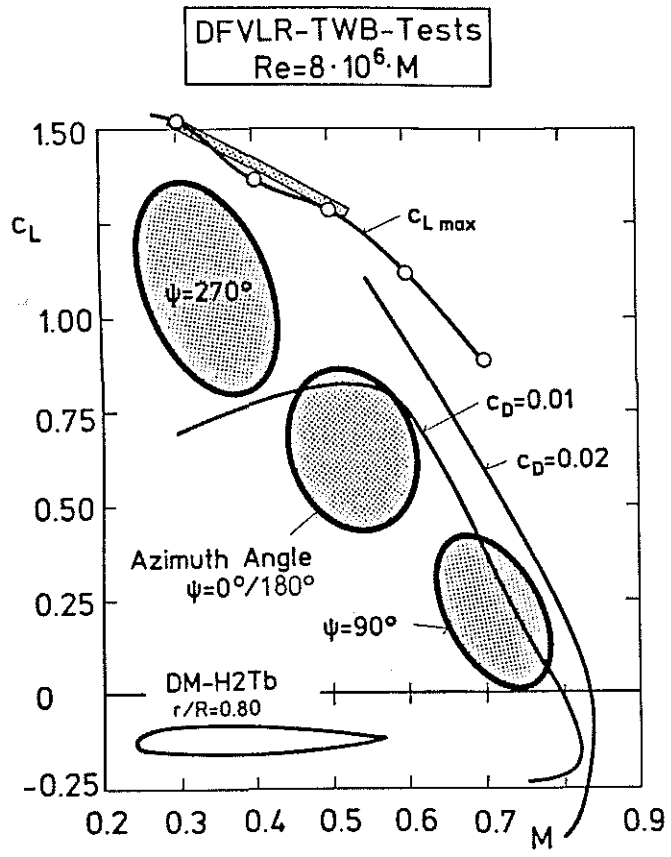

Fig. 1 Main operational conditions and measured performance boundaries for the inner airfoil

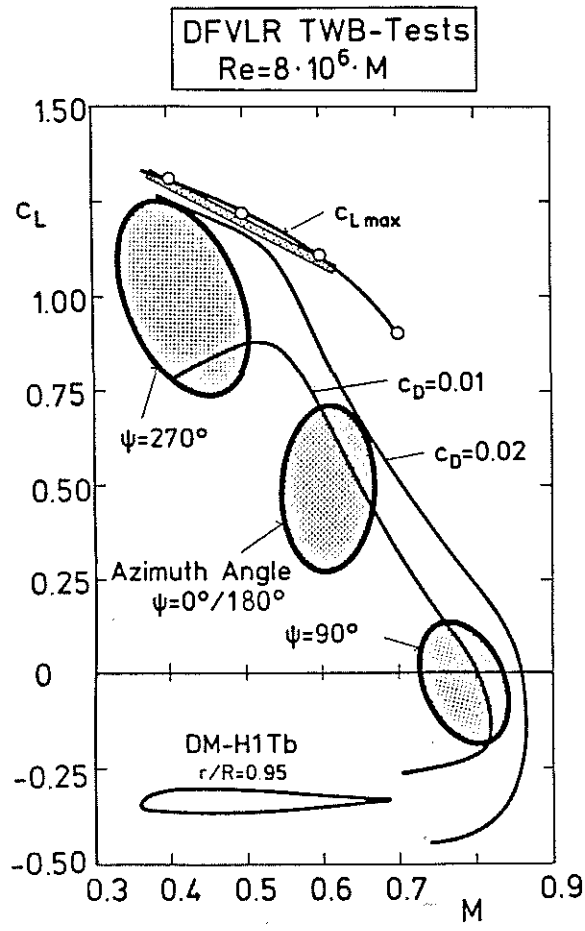

Fig. 2 Main operational conditions and measured performance boundaries for the tip airfoil

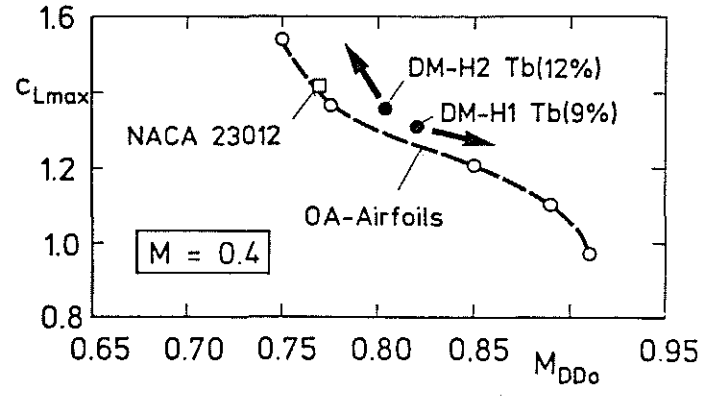

Fig. 3 Maximum lift coefficient versus drag divergence Mach number of several rotor blade airfoils at M = 0.4

DM-H1 Tb and DM-H2 Tb do not differ very much. To apply both airfoils useful in a rotor blade it is desirable to shift the values in the directions marked by the arrows.

Modifying the airfoils the same methods are used as described in reference [12]. For subsonic calculations a modified code from R. Eppler and D.M. Somers extended to subsonic flow [13], [14] has been used. This code bases on a conformal mapping procedure in its design part and on a higher order panel/boundary layer interaction method in its analysis part. For transonic flow the wellknown Bauer/Garabedian/Korn/Jameson method (BGK III) was used [15], [16] which also is coupled with a boundary layer method by adding the displacement thickness to the airfoil contour.

First the desired improvement of the maximum lift coefficient of the airfoil DM-H2 Tb at M = 0.4 may be discussed. The reliable prediction of maxi-

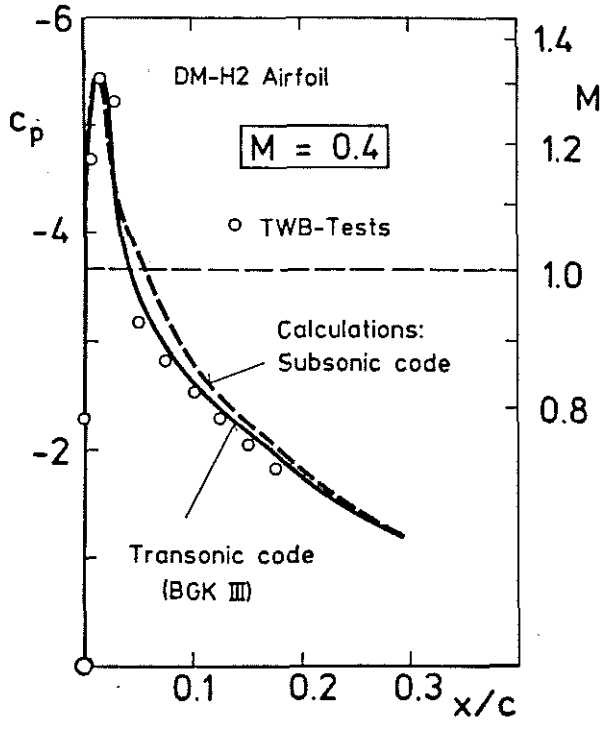

Fig. 4 Upper surface pressure distributions near the leading edge calculated with different methods and measured in the TWB

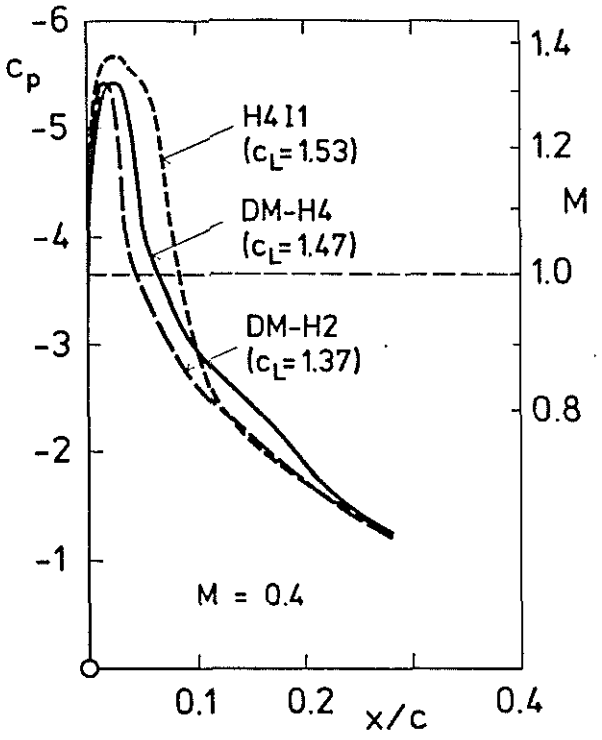

Fig. 5 Upper surface pressure distributions of several airfoils calculated with the BGK III-method [16]

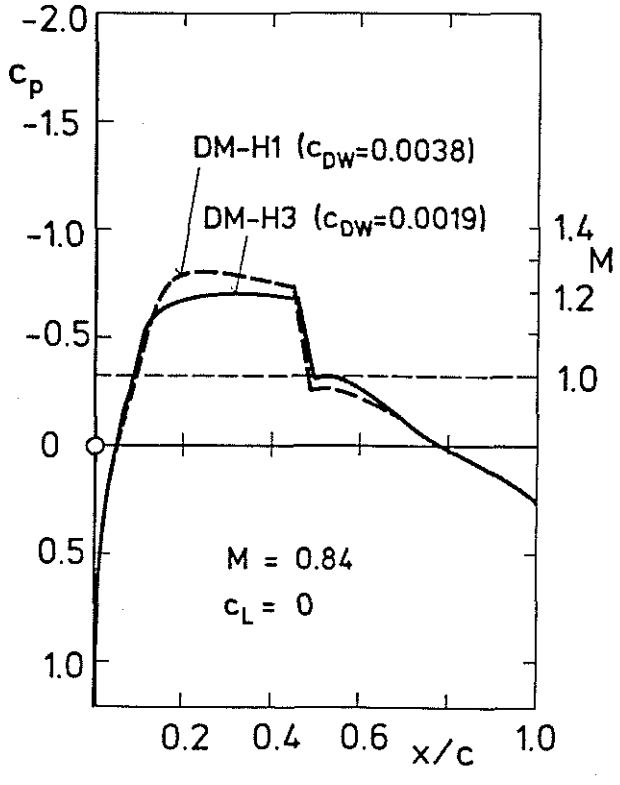

Fig. 6 Upper surface pressure distributions calculated by the BGK III-method [16]

mum lift coefficients in general is difficult. In the case of complete attached flow the usual potential flow/boundary layer interaction methods give satisfactory results. Near maximum lift, however, the flow in general is separated and additional empirical criterions are useful to estimate the maximum lift coefficient, e.g. to compare the calculated suction peak with experiments at similar airfoils, especially in the case of an additional turbulent separation bubble due to a shock at the end of a local supersonic zone. A further difficulty is illustrated in fig. 4, showing parts of pressure distributions of the airfoil DM-H2 calculated by the subsonic and the transonic code and measured in a windtunnel at M = 0.4 near maximum lift. The transonic calculation itself and also comparison of transonic and subsonic calculation give no indication of a shock, in contrast to the experiment, which shows a distinct shock. This lack of the transonic calculation may be caused by a non suffi-

cient number of grid points (161 on the airfoil contour are used in this case). It leads to a wrong boundary layer calculation, shifting the predicted maximum lift coefficient to a higher value and causing the dent in the $c_{L\,max}$-curve in fig. 1.

To improve the maximum lift coefficient a wellknown procedure, described for the Mach number M = 0.5 by several authors, [2], [3], has to be carried out. The small local supersonic flow field has to be extented as shown in fig. 5. This is attainable by a higher curvature near the end of the supersonic region and corresponding changes of curvature up- and downstream. This modification influences, of course, the aerodynamic characteristics at other operational points. Especially at higher Mach numbers an additional expansion of the supersonic flow in the region of the higher curvature is caused, followed by a stronger shock.

For the improved airfoil a moderate lift increase is chosen, marked by the solid curve in fig. 5. This is a good compromise for a smooth maximum lift coefficient curve for all the considered free stream Mach numbers and an only small reduction in the drag divergence Mach number at lower lift coefficients.

Just the opposite step has been done, modifying the thinner airfoil DM-H1 Tb. Fig. 6 shows the reduced local Mach numbers in the supersonic zone caused thereby and the resultant reduced wave drag calculated with the BGK III code.

The two modified airfoils provided with a tab and designated by DM-H3 Tb and DM-H4 Tb with a thickness to chord ratio t/c = 0.09 and 0.12 respectively are shown in fig. 7. The tab lengths amount to 5% of chord length for the DM-H3 Tb and to 4.5% for the DM-H4 Tb airfoil. The essential contour differences to the DM-H1 and DM-H2 airfoils are exhibited in fig. 8.

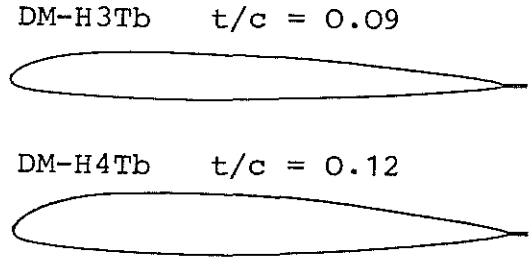

Fig. 7 Helicopter rotor blade airfoils DM-H3 Tb and DM-H4 Tb

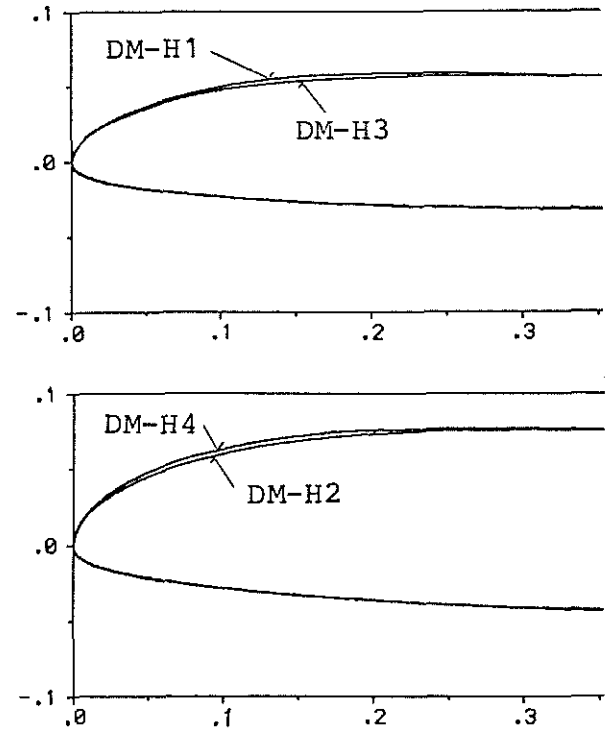

Fig. 8 The essential contour differences between the airfoils DM-H1, DM-H3 and DM-H2, DM-H4

3. Results

3.1 Windtunnel

The experimental investigations have been carried out in the Transonic Windtunnel Braunschweig (TWB) of the DFVLR [17]. The wind tunnel is of the blow-down type with a rectangular test section of 34 cm by 60 cm with slotted walls at the top and the bottom and is especially suited for airfoil tests at subsonic and transonic flows in the Mach number range of M = 0.3 to 0.9. All wind tunnel tests described in this paper have been carried out with natural transition at a Reynolds number of $Re = 8 \cdot 10^6 \cdot M$.

3.2 Experimental Results

The aim of the modification of the DM-H2 airfoil to raise the maximum lift coefficient at the Mach number of M = 0.4 has been attained as shown in fig. 9 presenting the maximum lift coefficient vers. Mach number of the airfoils DM-H2 Tb, DM-H4 Tb and OA 212.The maximum lift coeffient at M = 0.4 could be increased from $c_{L\,max}$=1.36 for the DM-H2 Tb airfoil to 1.53 for the DM-H4 Tb airfoil. In addition the $c_{L\,max}$-values for M = 0.3 and 0.5 could be raised considerably to $c_{L\,max}$=1.64 and 1.33 respectively. On the other hand the zero lift drag shown in fig. 10 increased for a small amount but the drag divergence Mach number defined by $dc_D/dM=0.1$ at c_L = 0 was not changed and is considerably higher than that of the OA 212 airfoil. The total performances of the DM-H4 Tb airfoil measured in the TWB are summarized in fig. 11 and compared with those of the DM-H2 Tb airfoil.

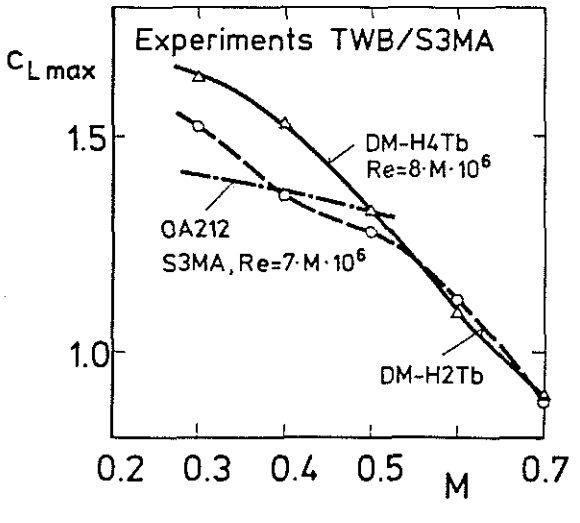

Fig. 9 Maximum lift coefficients of several airfoils with thickness to chord ratio t/c=0.12

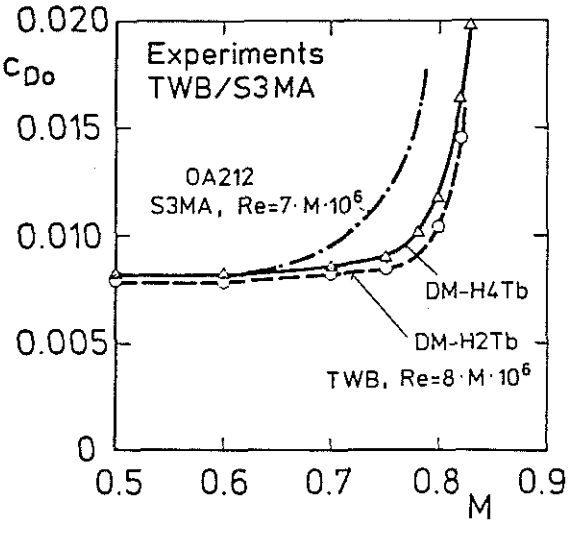

Fig. 10 Zero lift drag coefficients of several airfoils with thickness to chord ratio t/c = 0.12

The desired improvement of the high speed behaviour, especially the increase of the drag divergence Mach number for the DM-H3 Tb airfoil has been obtained and is shown in fig. 12. The drag divergence Mach number at zero lift could be raised from M_{DDo}=0.82 for the DM-H1 Tb airfoil to M_{DDo}=0.846 for the DM-H3 Tb airfoil. The decrease of the maximum lift coefficients shown in fig. 13 does not exceed the expected amount of Δc_L=0.05 and the $c_{L\,max}$ values of the DM-H3 Tb airfoil are larger than those of the OA 209 airfoil.

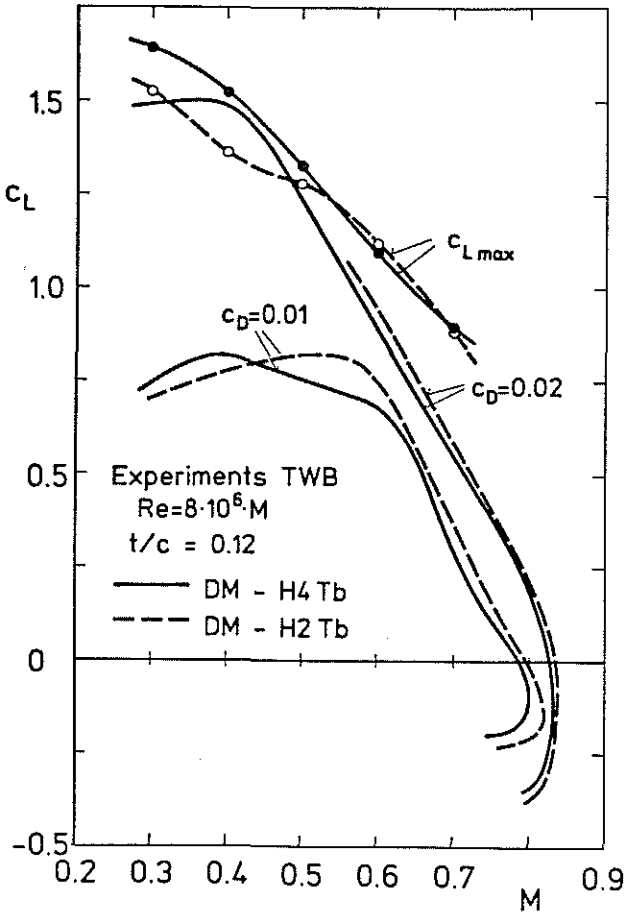

Fig. 11 Measured performance boundaries of the airfoils DM-H2 Tb and DM-H4 Tb

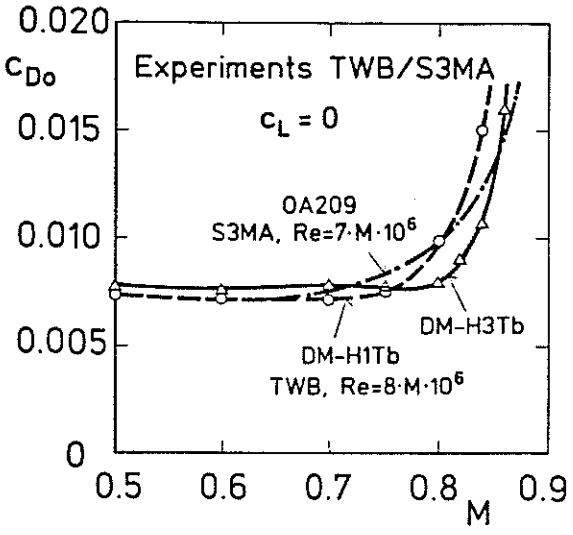

Fig. 12 Zero lift drag coefficients of several airfoils with thickness to chord ratio t/c = 0.09

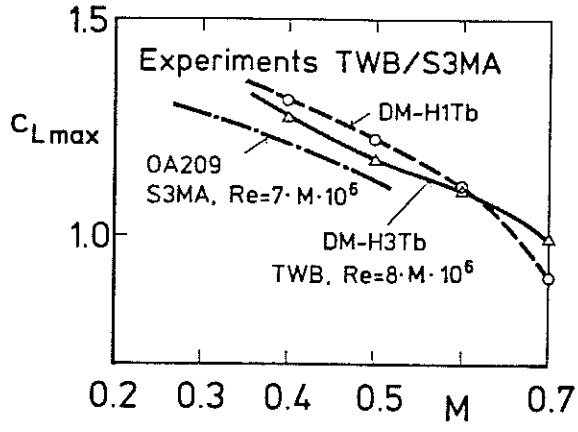

Fig. 13 Maximum lift coefficients of several airfoils with thickness to chord ratio t/c=0.09

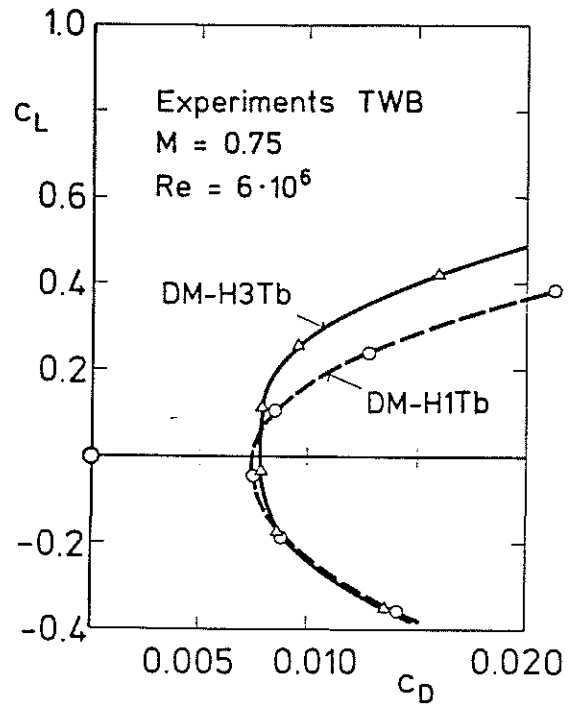

Fig. 14 Drag polars of the airfoils DM-H1 Tb and DM-H3 Tb

The main reason for the drag decrease at higher Mach numbers is the diminishing of the shock strength on the upper side of the DM-H3 Tb airfoil which first causes a smaller wave drag and second prevents the formation of a turbulent separation bubble behind the shock or at least reduces the length of the bubble. This is confirmed by the comparison of the two polar curves of the airfoils DM-H1 Tb and DM-H3 Tb at the Mach number of M = 0.75 on fig. 14.

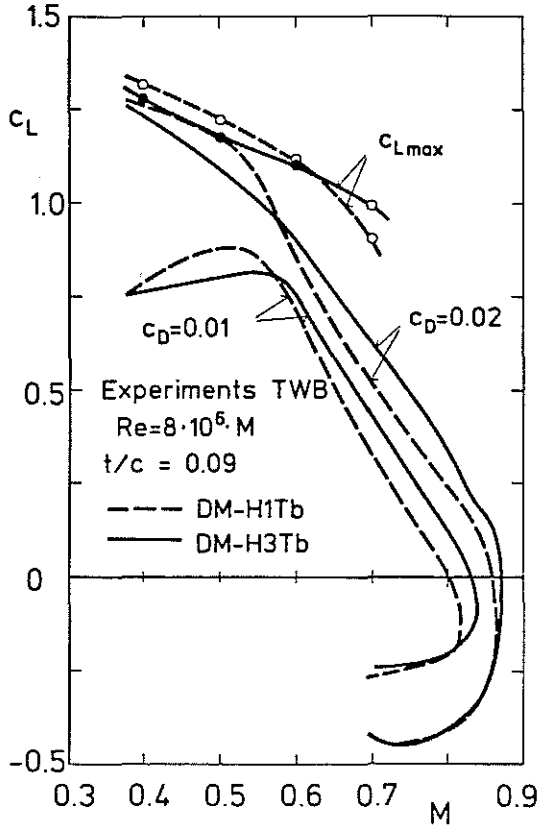

Fig. 15 Measured performance boundaries of the airfoils DM-H1 Tb and DM-H3 Tb

In the Mach number range of M = 0.6 to 0.85 the drag limits of c_D = 0.01 and 0.02 could be shifted to larger Mach numbers as can be seen in fig. 15 in which the total performances of the two airfoils DM-H1 Tb and DM-H3 Tb are presented.

The pitching moment coefficients at zero lift c_{mo} in dependance of Mach number of the considered airfoils are given in fig. 16. While the airfoils DM-H1 Tb and DM-H3 Tb show about the same behaviour, the DM-H4 Tb airfoil yields more negative values compared with the DM-H2 Tb which has been desired during the design process. The c_m evolution with lift coefficient at M = 0.4 on fig. 17 shows that the measured values essentially do not exceed ± 0.01 and that the tabs of the modified airfoils are more effective than those of DM-H1 Tb and DM-H2 Tb airfoils, that means the slope dc_L/dc_m is more negative.

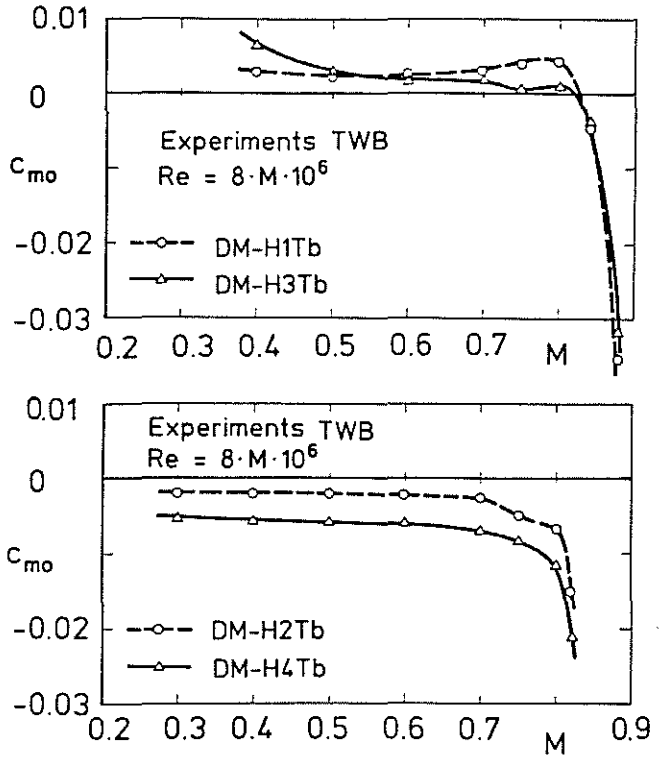

Fig. 16 Zero lift pitching moment for several airfoils

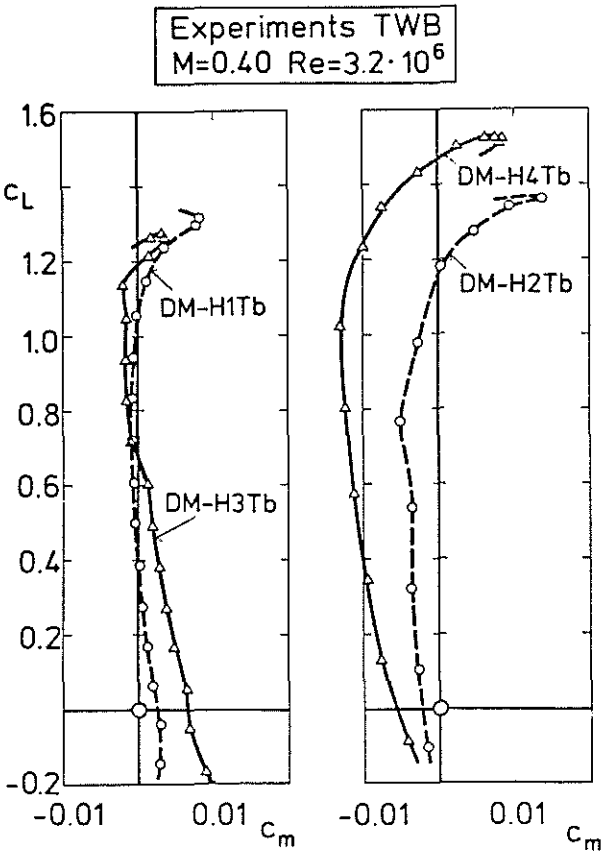

Fig. 17 Pitching moment evolution of several airfoils

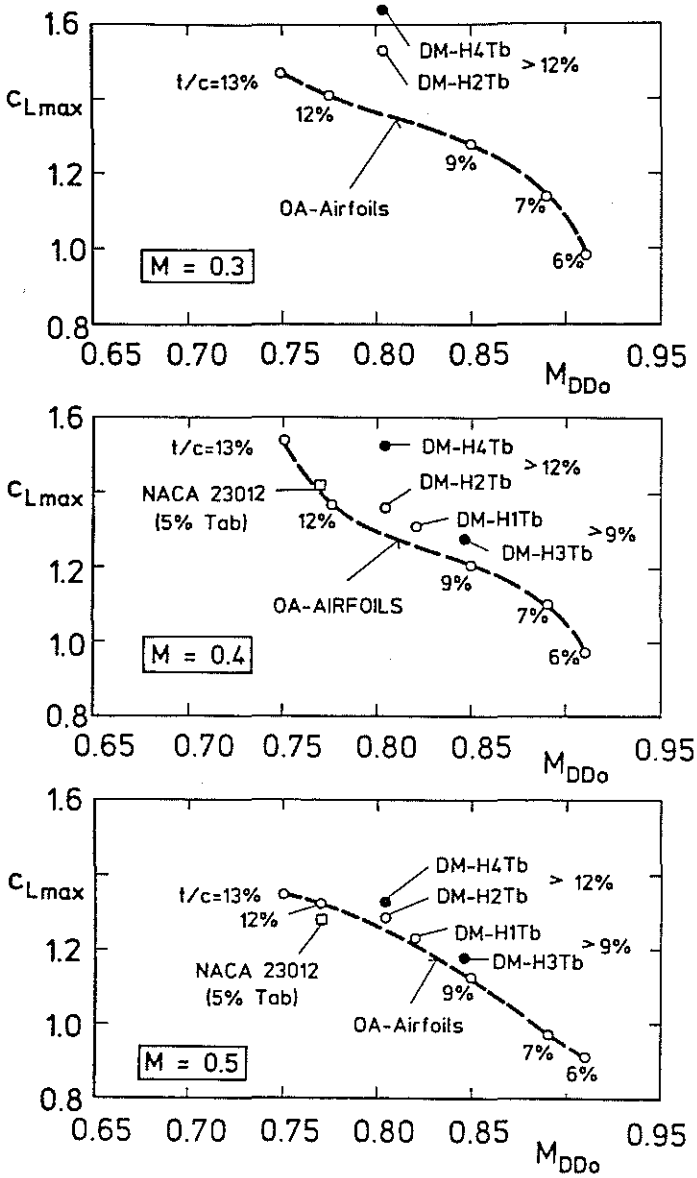

Fig. 18 Measured maximum lift coefficients and drag divergence Mach number at zero lift for several airfoils

A comparison of the DM-airfoils with the OA-series and the NACA 23012 (5% Tab) is presented in fig. 18 in maximum lift coefficient vers. drag divergence Mach number diagrams for the Mach numbers M = 0.3, 0.4 and 0.5. The desired gain in $c_{L\,max}$ for the DM-H4 Tb airfoil has been obtained especially for M = 0.4 and also for the other two Mach numbers without decreasing the drag divergence Mach number at zero lift. The shift of the drag divergence Mach number for the DM-H3 Tb airfoil has also been realized and the loss in maximum lift has been limited to $\Delta c_L = 0.05$.

The agreement between the calculated values of maximum lift and zero drag coefficients and the experimental results shown in fig. 19 and 20 is acceptable but does not replace accurate wind tunnel measurements.

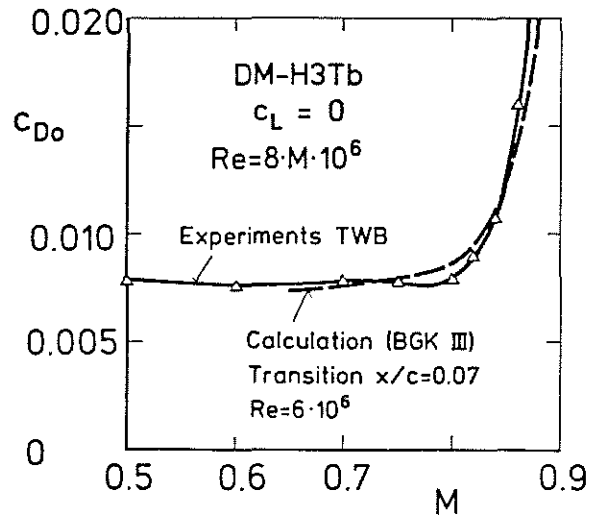

Fig. 19 Comparison of measured and calculated zero lift drag coefficients of the airfoil DM-H3 Tb

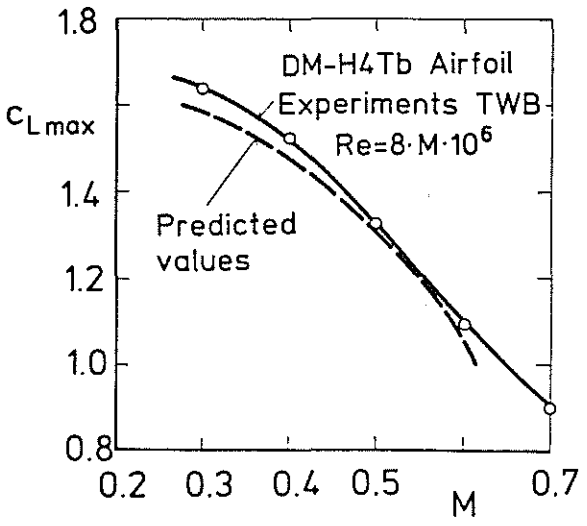

Fig. 20 Comparison of measured and predicted maximum lift coefficients of the airfoil DM-H4 Tb

4. Influence on helicopter performance and load factor capability

The useful effects of the modified airfoils DM-H3 Tb and DM-H4 Tb have been evaluated based on the BO 105 main rotor by theoretical comparison with respect to performance and load factor capability with the foregoing airfoils DM-H1 Tb and DM-H2 Tb as well as with the NACA 23012 airfoil, which is used on the BO 105 production rotor blades.

For the comparison of the new profile types, the 12% airfoils DM-H4 Tb, DM-H2 Tb are applied up to 80% radius, with a linear transition to the 9% airfoils DM-H3 Tb, DM-H1 Tb at the blade tip. The twist angle of -8 deg and the tip speed of 218 m/s is kept for the three rotor versions.

With the improved airfoils the figure of merit (fig. 21) is increased by about 1% compared to DM-H1 Tb/-H2 Tb and by 10% as against the NACA 23012 airfoil, thereby raising the F.M. to a maximum of 0.77.

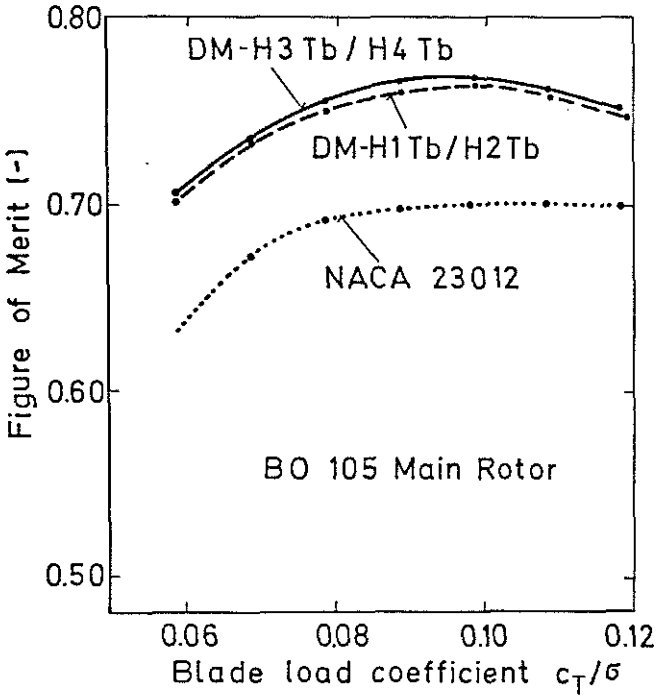

Fig. 21 Influence of blade airfoils on the figure of merit

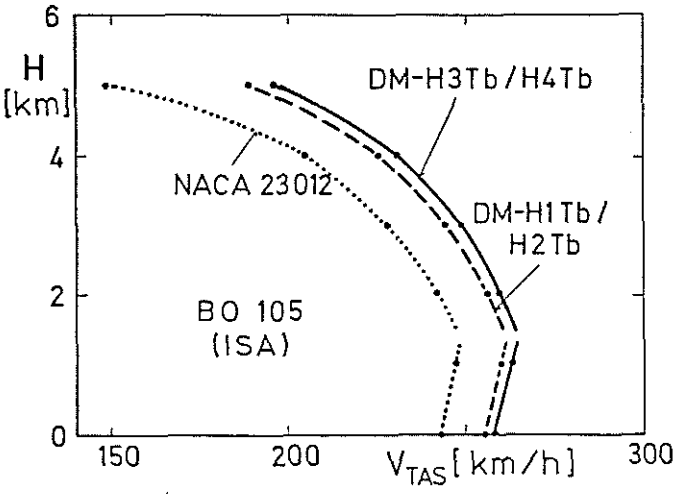

Fig. 22 Maximum cruise speed

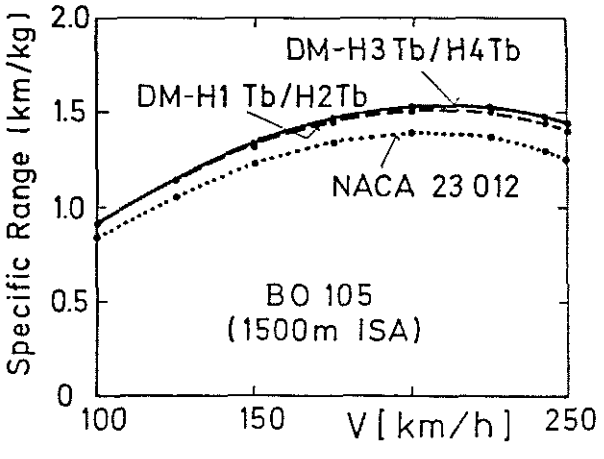

Fig. 23 Specific range

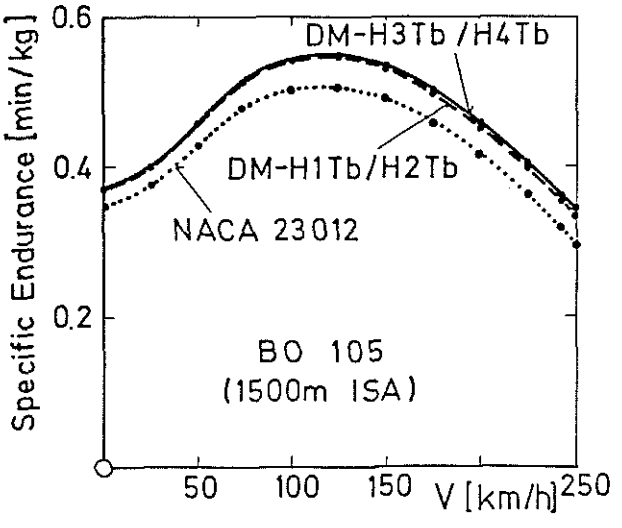

Fig. 24 Specific endurance

The maximum cruise speed (fig. 22) at low altitude is increased by about 3 km/h due to the improved airfoils and exceeds the figure of the actual NACA 23012 equipped rotor by 16 km/h. It should be noted that with increasing speed, not only the parasitic drag of the helicopter rises, but also the Mach number of the advancing blade is increased, both effects normally leading to higher power required. The advantages due to the improved airfoils become more significant at higher flight altitudes since the stall onset on the retreating blade, which affects also the power consumption of the rotor, is delayed by the higher maximum lift capability of the new airfoils.

Similar improvements were achieved in the specific range, which is increased by 2% over the DM-H1 Tb/-H2 Tb and 11% compared to the NACA 23012 in its optimum (fig. 23). The advantage of the modern airfoils is more evident with increasing flight speed, so that also the flight speed for optimum range is increased. However, it must be said, that from a profile design point of view the optimum range state is characterized by only moderate conditions on both the Mach numbers on the advancing blade and the high lift coefficients on the retreating blade. Nevertheless for the operator reductions in specific fuel consumption can be turned into useful payload, hence reducing the overall operating costs.

Similar advantages are to be seen at the optimum endurance flight condition (fig. 24), whereby improvements of 0.5% compared to the DM-H1 Tb/-H2 Tb profiles and 10% over the NACA 23012 are obtained.

At the flight speed of optimum rate of climb which is close to the optimum endurance speed, a nearly constant increase in the optimum rate of climb of 0.2 m/sec respectively 1.2 m/sec is achieved over the whole altitude range (fig. 25).

The maximum load factor envelope (fig. 26) of the BO 105 rotor is also improved by the new airfoils. The advantage, compared with the former airfoils DM-H1 Tb/-H2 Tb, mainly comes from the increase in maximum lift capability of the DM-H4 Tb airfoil at the inner blade section. Due to the improved airfoils the maximum load factor is increased by .2g over the DM-H1 Tb/-H2 Tb and .4g over the NACA 23012. Correspondingly the maximum achievable speed for a specific load factor is increased.

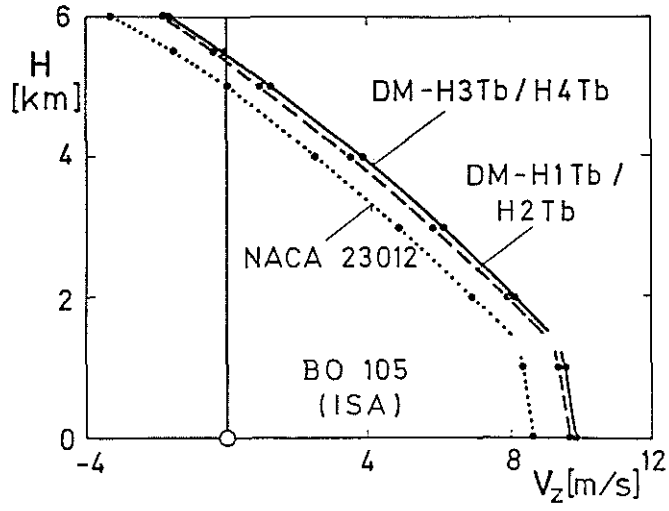

Fig. 25 Maximum rate of climb

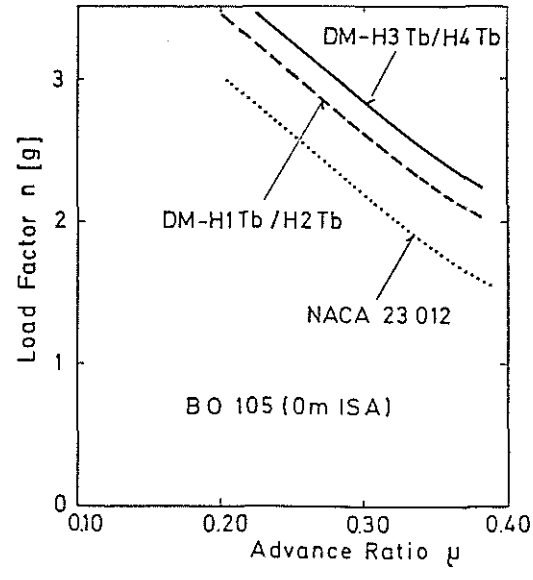

Fig. 26 Load factor capability

Summary

The rotor airfoils DM-H1 Tb and DM-H2 Tb resulting of a cooperation between MBB and DFVLR are improved in a second development step. Aims and features of desired modifications as well as contour changes are discussed.

At the inner airfoil the maximum lift coefficient at M = 0.4 should increase and the drag rise of the blade tip airfoil should be shifted to higher Mach numbers. The new airfoils designated by DM-H3 Tb and DM-H4 Tb are investigated in the windtunnel. The presented results show that the desired improvements are obtained. The maximum lift coefficients of the airfoil DM-H4 Tb raise up to values of $c_{L\ max}$=1.64, 1.53 and 1.33 at Mach numbers M = 0.3; 0.4 and 0.5 respectively. The reduction of drag rise Mach numbers are very small.

The drag divergence Mach number at zero lift of the DM-H3 Tb airfoil is shifted to a value of M_{DDo}=0.846 while the maximum lift coefficients are slightly reduced to values of $c_{L\ max}$=1.28 and 1.18 at the Mach numbers M = 0.4 and 0.5 respectively.

From the comparison, based on the BO 105 rotor, it has been demonstrated that significant improvements are to be found at all flight conditions with the new DM-H3 Tb/-H4 Tb airfoils, when compared with the initial DM-H1 Tb/-H2 Tb advanced airfoil design and the classical NACA 23012 profile.

References

[1] G. Reichert and S.N. Wagner, Some Aspects of the Design of Rotor Airfoil Shapes, AGARD-CP-111, 1973, Paper 14.

[2] F.X. Wortmann, J.M. Drees, Design of Airfoils for Rotors, Paper presented at the CAL/AVLABS 1969 Symposium on Aerodynamics of Rotary Wing and VTOL Aircraft, Buffalo, N.Y..

[3] J.W.Sloof, F.X. Wortmann, J.M. Duhon, The Development of Transonic Airfoils for Helicopters, Paper presented at the 31st Annual National Forum of the American Helicopter Society, Washington D.C., May 1975.

[4] R.W. Prouty, A State-of-the-Art Survey of Two-Dimensional Airfoil Data. AHS Symposium on Helicopter Aerodynamic Efficiency, March 1975.

[5] J. Renaud and F. Nibelle, Effects of the Airfoil Choice on Rotor Aerodynamic Behaviour in Forward Flight. Paper presented at the 2nd European Rotorcraft and Powered Lift Aircraft Forum, Bückeburg, September 1976.

[6] L. Dadone, Rotor Airfoil Optimization: An Understanding of the Physical Limits, Paper presented at the 34th Annual National Forum of the American Helicopter Society, May 1978, Washington D.C., Preprint 78-4.

[7] J.J. Thibert and J. Gallot, A New Airfoil Family for Rotor Blades, Paper presented at the 3rd European Rotorcraft and Powered Lift Aircraft Forum, Paper No. 41, Aix-en-Provence, September 1977, T.P. ONERA 1977-131.

[8] J.J. Thibert and J. Gallot, Advanced Research on Helicopter Blade Airfoils, Paper presented at the 6th European Rotorcraft and Powered Lift Aircraft Forum, Paper No. 49, Bristol, September 1980, T.P. ONERA 1980-93.

[9] J.J. Thibert and J.M. Pouradier, Design and Test of a Helicopter Rotor Blade with Evolutive Profile, 12th ICAS Congress, Munich, October 1980, T.P. ONERA 1980-125.

[10] L. Dadone, The Role of Analysis in the Aerodynamic Design of Advanced Rotors, AGARD-CPP-334, Paper 1, May 1982.

[11] J.J. Thibert and J.J. Philippe, Etudes de Profiles et d'Extrémités de Pale d'Hélicoptère, AGARD-CPP-334, Paper 3, May 1982.

[12] K.H. Horstmann, H. Köster, G. Polz, Development of Two Airfoil Sections for Helicopter Rotor Blades. Z. Flugwissen. Weltraumforsch. 7(1983), pp. 82-91; Paper presented at the Eight European Rotorcraft Forum, Aix-en-Provence, France, August 31st to September 3rd, 1982.

[13] R. Eppler and D.M. Somers, A Computer Program for the Design and Analysis of Low-Speed Airfoils, NASA TM 80210, 1980.

[14] R. Radespiel, Erweiterung eines Profilberechnungsverfahrens im Hinblick auf Entwurfs- und Nachrechnungen von Laminarprofilen bei Verkehrsflugzeugen, DFVLR IB 129-81/15, 1981.

[15] F. Bauer, P. Garabedian, D. Korn, A. Jameson, Supercritical Wing Sections II, Springer-Verlag, Berlin, Heidelberg, New York, 1975.

[16] F. Bauer, P. Garabedian, D. Korn, Supercritical Wing Sections III, Springer-Verlag, Berlin, Heidelberg, New York, 1977.

[17] E. Stanewsky, W. Puffert-Meißner, R. Müller, H. Hoheisel, Der Transsonische Windkanal Braunschweig der DFVLR, Z. Flugwissen. Weltraumforsch. 6(1982), pp. 398-408.